

On Statistical Properties of CMEs Associated with Prominence Eruption

Veerendra Singh

Associate Professor, Deptt. of Physics, Meerut College, Meerut-250001, Uttar Pradesh, India

Lavkush Kumar

Associate Professor, Deptt. of Physics, R. H. Government, P.G. College, Kashipur-244713, Uttarakhand, India

Abstract: In this paper we have made a comprehensive statistical study on the CMEs associated with prominence eruptions. A total number of 576 prominence eruptions observed by Nobeyama Radioheliograph during the period January, 1996 to December, 2013. We have studied the distribution of CMEs speed, angular width and acceleration for prominence eruptions associated CMEs. The median (average) linear speed is 492 (521) km/sec. The mean angular width is 77° . Majority of events is accelerating. On studying the speed-acceleration correlation for these events we found there is no correlation between them. The number variation during solar cycle of prominence activities is similar to that of sunspots. The fraction of prominence eruptions associated CMEs during the solar minimum is less than that during solar maximum. We have also studied the mass, energy and latitudinal distribution of prominence eruptions associated CMEs.

Index Terms: Sun; Coronal Mass Ejections; Prominence Eruptions; Solar cycle

1. Introduction

Coronal mass ejections (CMEs) are often seen as spectacular eruptions of matter from the Sun, which propagate outward through the heliosphere and often interact with the Earth's magnetosphere (Hundhausen, 1997; Mittal and Narain, 2010 & references therein). It is well known that these interactions can have substantial consequences on the geomagnetic environment of the Earth, sometimes resulting in damage to satellites (Mittal et al., 2010). A bright core in the three part classical structure of CME is the remnant of an eruptive prominence (Crifo et al., 1983; Illing and Hundhausen, 1985; Mittal and Narain, 2010).

Prominence eruptions (PE) are one of the earliest known forms of mass ejections from the Sun since the late 1800's (Tandberg- Hanssen, 1995). Two primary types of mass motions have been recognized in prominences, one with material streaming from one part of the solar surface to another (active prominences) and the other with prominence material leaving the Sun partially or completely (eruptive prominences). It is well established that quite often prominence eruptions are associated with coronal mass ejections. Laura et al. (2014) studied the evolution of two erupting prominences associated to CMEs using combined data from ground and space. We have also compared these observations with the model by Chen (1996) of the eruption of a flux rope and found good agreement. [McCauley](#) et al. (2015) studied the prominence and filament eruptions observed by the Atmospheric Imaging Assembly (AIA) onboard the Solar Dynamics Observatory (SDO) and found that the average fast-rise onset height, slow-rise duration, slow-rise velocity, maximum field-of-view (FOV) velocity, and maximum FOV acceleration are 83 Mm, 4.4 hours, 2.1 km/s, 106 km/s, and 111 m/s, respectively. Several authors have been made detailed studies about prominences and CMEs yet (Tandberg-Hanssen 1995, 2011, Gopalswamy et al., 2003, Gopalswamy, 2006, Mittal and Narain, 2009, Gupta et al., 2014 and references therein).

In view of above it seems worthwhile to make a detailed study of CMEs associated with prominence eruption of SOHO era. In this paper we have studied properties of CMEs those associated with PEs in brief. We have studied variation of speed, angular width, their acceleration, latitudinal position, mass and energy and also study their annual variation with sun spots.

2. Data, Results and Discussion

Over the past 18-years the SOHO/LASCO instrument has been detecting CMEs. From Jan. 1996 to Dec. 2013, more than 23000 CMEs have been observed by SOHO/LASCO. During the period total 576 Prominence Eruption events have been taken from Nobeyama Radioheliograph which observes the Sun in two frequencies, 17 GHz and 34 GHz. The LASCO instrument (Brueckner et al., 1995) consists of three coronagraphs C1, C2 and C3 which images the corona in successively C1: 1-1.3R_s, C2: 2-6R_s; C3: 3.8-32R_s. The combined field of view of LASCO enables one to investigate the full kinematical evolution of CMEs. The height-time data of CMEs used in this study are taken from the online SOHO/LASCO CME catalogue (http://cdaw.gsfc.nasa.gov/CME_list), in which CME kinematics are estimated from LASCO C2 and C3 images. Out of 576 PEs 373 are associated with CMEs.

The speed distribution of CMEs those associated with PEs has been shown in Figure 1. Figure 1 shows linear speed distribution of events. It shows that the peak of the histogram occurs at 550 km/sec but the tail of large speeds is short. The overall median (average) speed is 492 (521) km/sec., respectively.

As the position angle extent in the sky plane, CMEs width is measured. Many CMEs show an increase in width as they move out, so measurements are made when the width appears to approach a constant value.

Figure 2a is the histogram of apparent angular width for the period 1996–2013. The average width from the 18-year data involving 373 CMEs those associated with PEs is 77° and the median width is 46°.

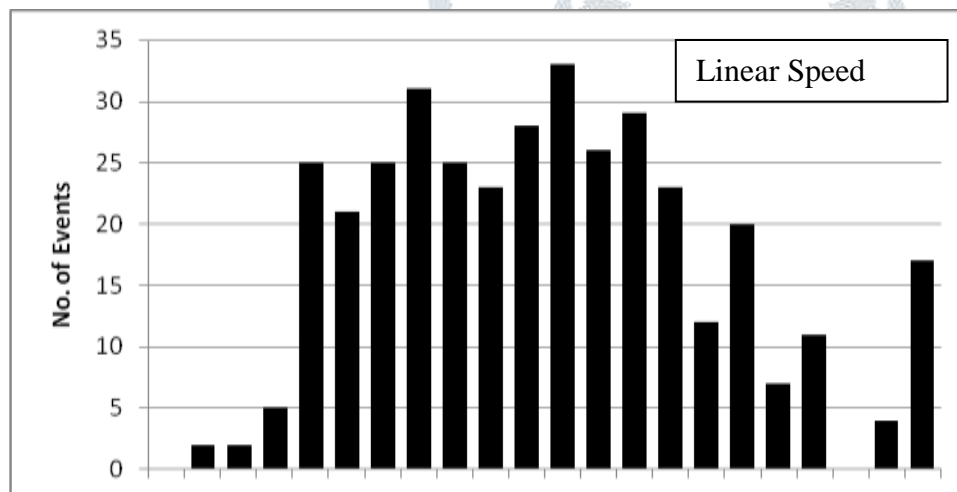


Figure 1: Histogram shows the linear speed distribution of CMEs those associated with PEs during 1996–2013.

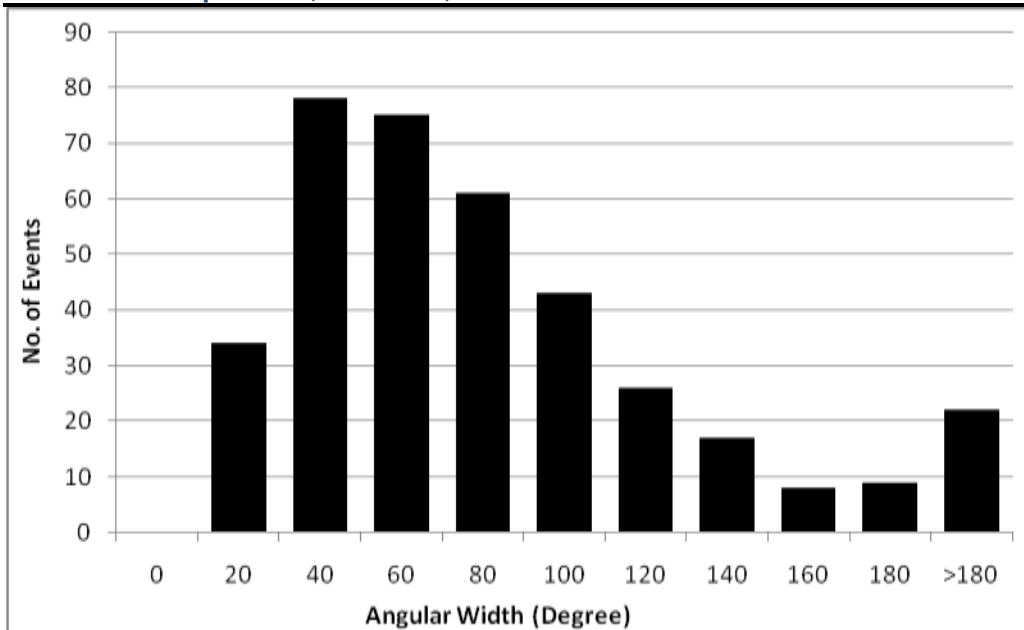


Figure 2a: The width distribution of SOHO/LASCO Prominence Eruption associated CMEs from 1996 to 2009. The last bin shows all CMEs with width $>180^\circ$, which amounts to 5–6% of all Prominence Eruption associated CMEs.

In Figure 2b we show relation between CMEs speed and apparent angular width. It is clear from figure that at higher angular width average speed is high in compare to low angular width.

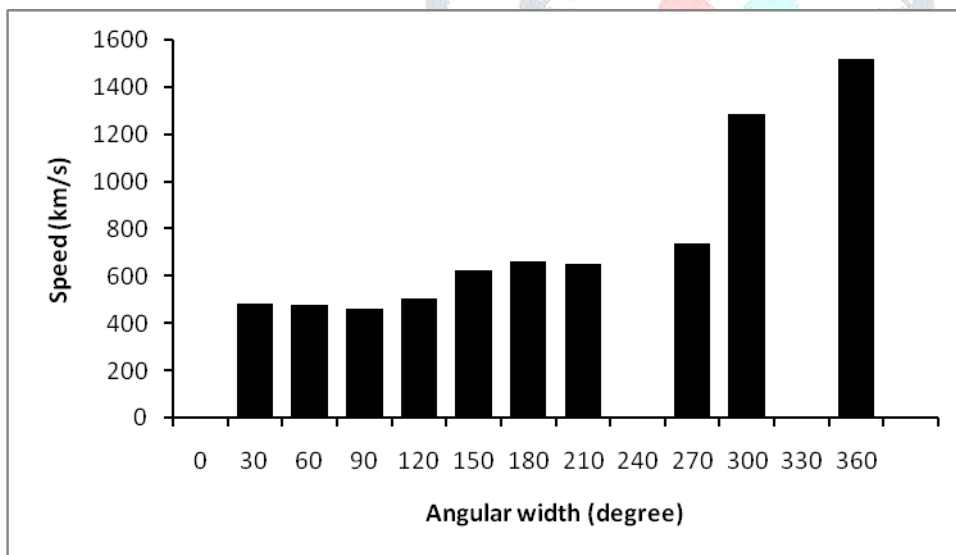


Figure 2b: Histogram shows average speed for apparent angular width.

Figure 3 is the histogram of 367 out of 373 CMEs those associated with PEs acceleration for the period 1996–2013. The fractions in each 5 km/s^2 interval are plotted. It is clear from this figure that a majority (52%) of CMEs associated with PEs are accelerated, about 9% of them move with little acceleration and the remaining 39% have negative acceleration. Thus CMEs associated with PEs have clear bias towards positive acceleration.

Figure 4 shows a scatter plot between the measured acceleration, a (in m/s^2) and speed, V (in km/s) of prominence eruption associated CMEs for which the acceleration estimate was possible.

It is clear from figure that there is no correlation between acceleration and speed of PEs associated CMEs.

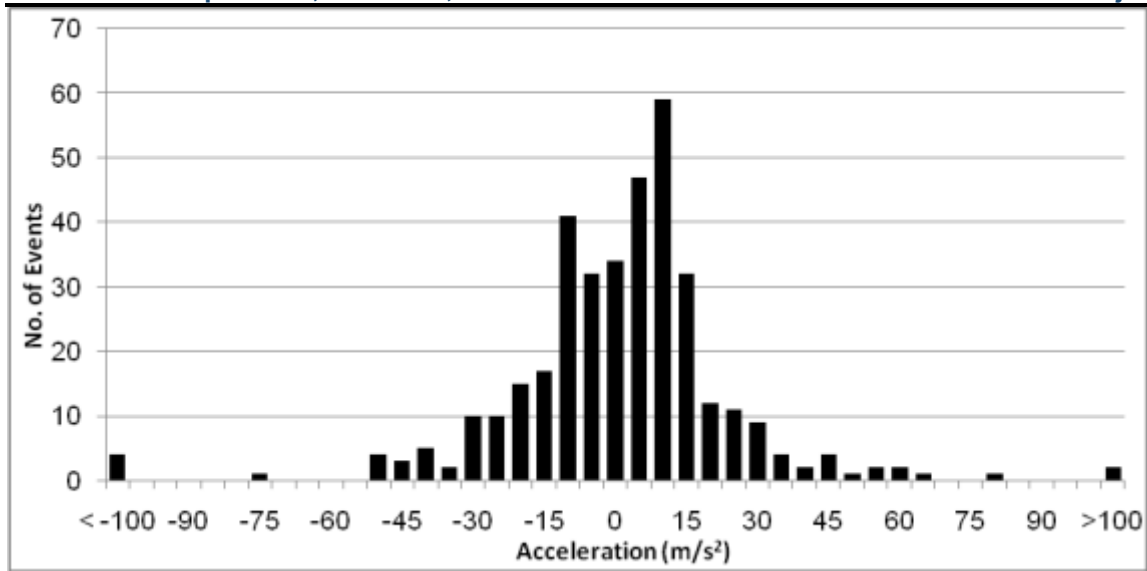


Figure 3: Histogram of acceleration of PEs associated CMEs, showing clear bias towards acceleration.

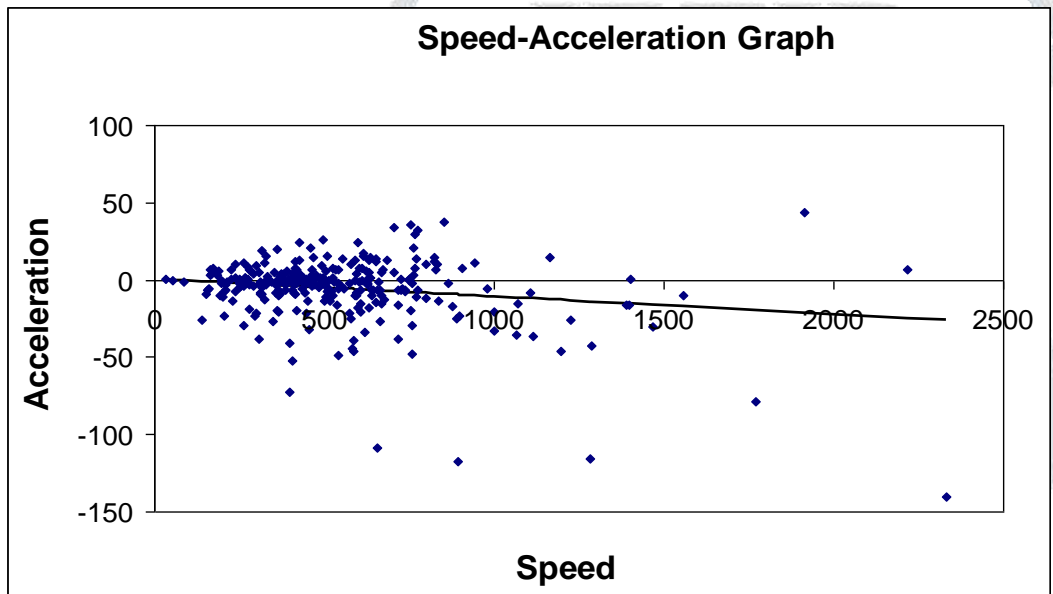


Figure 4: Acceleration as a function of speed of Prominence Eruption associated CMEs from 1996 to 2013. The acceleration has a large scatter, but there is a clear trend that the fast CMEs decelerate, while slow CMEs accelerate/decelerate.

The latitudinal distribution of CMEs depends on the distribution of closed magnetic field regions on the solar surface. CMEs propagate radially away from the solar source region on the basis of this assumption the latitude of CMEs can be obtained from central position angle (Hundhausen, 1994; Gopalswamy, et al., 2003). During solar minimum this assumption may not be valid because the CME path may be controlled by the global dipolar field of the Sun.

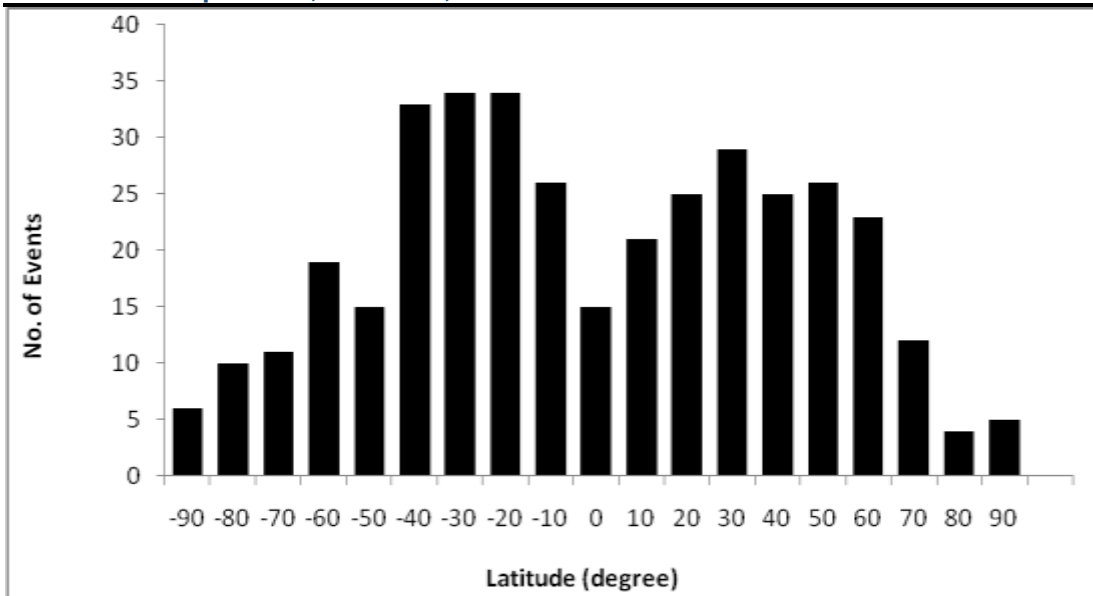


Figure 5: Histogram shows the latitude distribution of CMEs those associated with Prominence Eruption from 1996 to 2013.

During solar minimum CMEs tend to come from regions focused at or near the solar equator. Since at solar maximum, CMEs comes from a larger spread of solar latitudes, hence they have direct association with other coronal features.

Figure 5 shows distribution of apparent latitude for the 18-year (1996–2013) period involving 373 CMEs those associated with PEs. It is clear from Figure 7 that a very few CMEs (4%) are ejected from close to the equator. About 46% originate from northern hemisphere and 50% originate from southern hemisphere. So we can say the distribution is almost symmetrical about the equator. During 1996–2013 the number of Prominence Eruption associated CMEs having latitudes in between $\pm 10^0$ and $\pm 40^0$ is much larger than those beyond $\pm 40^0$.

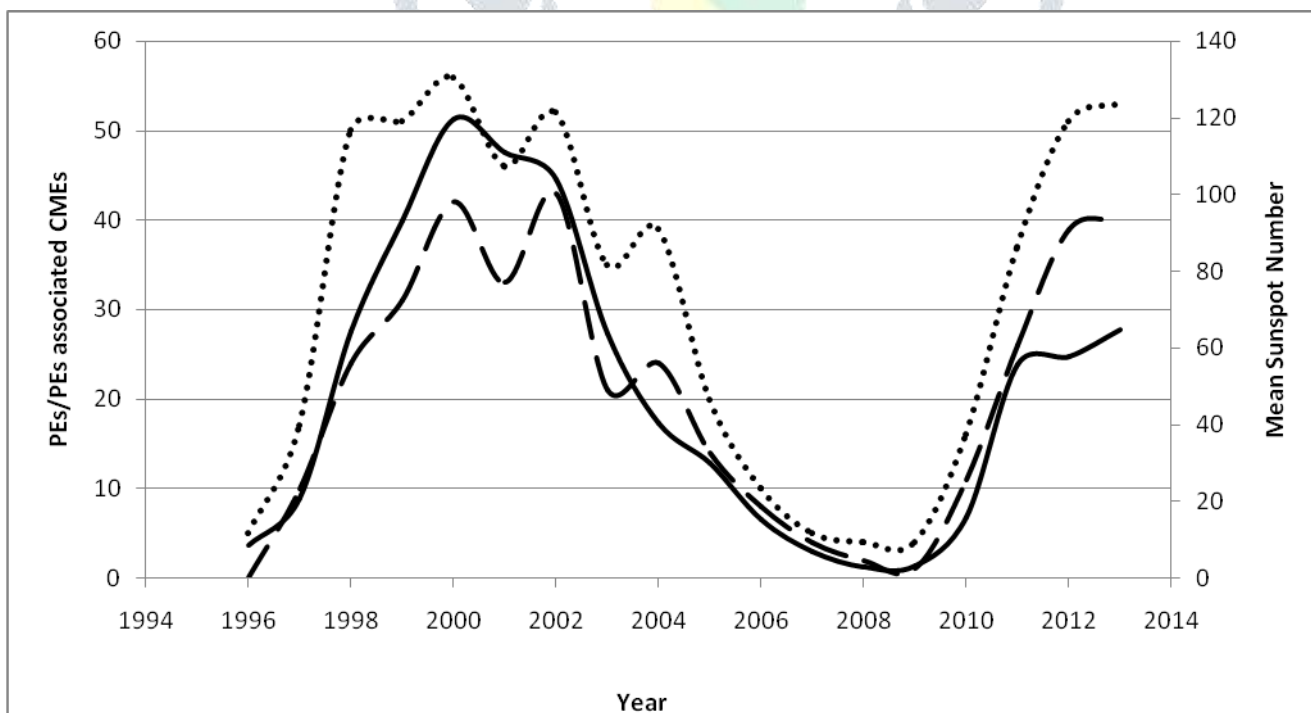


Figure 6: Comparison between annual occurrence rate of PEs associated CME, Prominence Eruptions and mean sunspot from 1996-2013. Solid line represents mean sunspot number; dotted line represents Prominence Eruptions while the dashed line is for CMEs those associated with PEs.

Figure 6 exhibits total PEs associated CMEs, PEs and mean sunspot number. It is clear from the figure that the solar maximum peak occurs at the year 2000 and 2002 during solar cycle 23. The number of sunspot (119) and PEs (56) is maximum in year 2000 while in year 2002 the number of sunspot (104) and PEs (52). Occurrence of PEs associated CMEs is maximum in 2002 (43) in compare to year 2000 (42). During solar cycle 24 peaks occurs at the year 2013 which is maximum phase of solar cycle 24. In year 2013 the number of sunspot (65), PEs (53) and PEs associated CMEs (40). From figure it is clear that occurrence rate of Prominence Eruptions and PEs associated CMEs follows the solar cycle variation. Occurrence rate is minimum during 2007-2009 due to deep solar minimum. During this period all solar activities are very minimum.

3. Conclusions

The data base can be used for a variety of statistical analyses. In this paper, we have made a comprehensive statistical study on CMEs those associated with Prominence Eruption from 1996 to 2013. During the period 1996-2013 more than 23000 CMEs observed by SOHO/LASCO, whereas Nobeyama Radioheliograph detected 576 prominence eruption events, out of which 373 Prominence Eruptions are associated with CMEs. So we presented our preliminary analysis of a sample of 373 LASCO CMEs that were associated with prominence eruptions during 1996-2013.

1. Figure 1 shows that the CMEs those associated with PEs have median (average) linear speed 492 (521) km/s. The number of prominence eruption associated CMEs having speeds greater than 1000 km/s is quite small (4-7%).
2. The average width for CMEs those associated with PEs is 77° and the median width is 46° .
3. At high angular width average speed is much high in compare to lower widths.
4. The acceleration distribution shows a conspicuous peak near 10 m/sec^2 . About 52% have positive acceleration, 39% have negative acceleration and the remaining 9% have very little acceleration. The Prominence Eruption associated CME distribution is biased towards acceleration.
5. About 46% of all CMEs come from northern hemisphere and about 50% come from southern hemisphere. Only 4% of CMEs come from equatorial region.
6. Rate of Prominence Eruptions varies with solar cycle.

Acknowledgement: I am thankful to authorities of Meerut College, Meerut for providing the facilities for this work. The CME catalog is generated and maintained at the CDAW Data Center by NASA and The Catholic University of America in cooperation with the Naval Research Laboratory. SOHO is a project of international cooperation between ESA and NASA. The authors would like to thank for the excellent LASCO-CME catalogue, which includes supportive data the back-bone of our paper. Authors are also thankful to Nobeyama Radioheliograph organization for providing the prominence eruption data.

References

1. Brueckner, G.E., Howard, R.A., Koomen, M.J., et al.: Sol. Phys., 162, 357, (1995)
2. Chen, J., JGR, 101, 27499, (1996)
3. Crifo, F., Picat, J. P., & Cailloux, M., Sol. phys, 83, 143, (1983)
4. Gopalswamy, N.: Astrophys. Astron., 27, 243 (2006)
5. Gopalswamy, N., Shimojo, M., Lu, W., Yashiro, S., Shibasaki, K., Howard, R.A.: Astrophys. J.

586, 562–578 (2003)

6. Gopalswamy, N., Mikic, Z., Maia, D., Alexander, D., Cremades, H., Kaufmann, P., Tripathi, D. & Wang, Y.-M., SSR, 123, 303, (2006)
7. Gupta, P., Gupta, M., Yadav, R., Narain, U., Astrophysics and Space Science 352, 395 (2014)
8. Hundhausen, A. J., Burkepile, J. T., & St. Cyr, O. C., JGR, 99, 6543, (1994)
9. Hundhausen, A.J.: In: Many Faces of the Sun: a summary of the results from NASA's Solar Maximum Mission, Eds: Strong, K.T., Saba, J.L.R., Haisch, B.M., p. 143. Springer, New York (1999)
10. Illing, R. M. E. & Hundhausen, A. J., JGR, 90, 275, (1985)
11. Laura, B. A. ; Cremades, H. ; Stenborg, G. ; Francile, C.; Di Lorenzo, L. and López, F., Nature of Prominences and their role in Space Weather. Edited by Brigitte Schmieder, Jean-Marie Malherbe and S. T Wu. Proce. of the International Astronomical Union, IAU Symposium, 300, 179, (2014)
- 12.. McCauley, P. I. ; Su, Y. N. ; Schanche, N. ; Evans, K. E. ; Su, C. ; McKillop, S. and Reeves, K. K. Solar Physics, 290 (6), 1703, (2015)
13. Mittal, N. and Narain, U., New Astron. 14, 341 (2009)
14. Mittal, N. and Narain, U., J. Atmos. Sol.-Terr. Phys., 72, 643 (2010)
15. Tandberg-Hanssen, E., The Nature of Solar Prominences. Kluwer, Dordrecht (1995)
16. Tandberg-Hanssen, E., Sol. Phys., 269, 237, (2011)
17. Webb, D. F. and Howard, R. A., JGR, 99, (A3), 4201, (1994)
18. Yashiro, S., Gopalswamy, N., Michalek, G., Rich, N., St. Cyr, C.O., Plunkett, S.P., Howard, R.A.: J. Geophys., 109, A07105 (2004)

